JOURNAL OF VIROLOGY, May 1985, p. 329–336
0022-538X/85/050329-08$02.00/0

Vol. 54, No. 2

Structure of the Intracellular Defective Viral RNAs of Defective Interfering Particles of Mouse Hepatitis Virus

SHINJI MAKINO,†* NOBORU FUJIOKA, AND KOSAKU FUJIWARA

Department of Animal Pathology, Institute of Medical Science, University of Tokyo, 4-6-1, Shirokanedai, Minato-ku, Tokyo 108, Japan

Received 6 September 1984/Accepted 22 January 1985

The intracellular defective RNAs generated during high-multiplicity serial passages of mouse hepatitis virus JHM strain on DBT cells were examined. Seven novel species of single-stranded polyadenylic acid-containing defective RNAs were identified from passages 3 through 22. The largest of these RNAs, DIssA (molecular weight [mw], 5.2 × 10^6), is identical to the genomic RNA packaged in the defective interfering particles produced from these cells. Other RNA species, DIssB1 (mw, 1.9 × 10^6 to 1.6 × 10^6), DIssB2 (mw, 1.6 × 10^6), DIssC (mw, 2.8 × 10^6) DIssD (mw, 0.82 × 10^6), DIssE (mw, 0.78 × 10^6), and DIssF (mw, 1.3 × 10^6) were detected at different passage levels. RNase T_1-resistant oligonucleotide fingerprinting demonstrated that all these RNAs were related and had multiple deletions of the genomic sequences. They contained different subsets of the genomic sequences from those of the standard intracellular mRNAs of nondefective mouse hepatitis virus JHM strain. Thus these novel intracellular viral RNAs were identified as defective interfering RNAs of mouse hepatitis virus JHM strain. The synthesis of six of the seven normal mRNA species specific to mouse hepatitis virus JHM strain was completely inhibited when cells were infected with viruses of late-passage levels. However, the synthesis of RNA7 and its product, viral nucleoprotein, was not significantly altered in late passages. The possible mechanism for the generation of defective interfering RNAs was discussed.

Over the last few years many of the steps in the replication of coronaviruses, particularly mouse hepatitis virus (MHV) and infectious bronchitis virus, have been elucidated (30, 31). The genomic RNA of MHV encodes RNA-dependent RNA polymerases (2, 3, 17), which are responsible for the synthesis of a genome-sized negative-stranded RNA (12). The negative-sensed RNA then serves as the template for the synthesis of both six species of subgenomic mRNAs and a genome-sized RNA (1, 12). These mRNAs are arranged in the form of a 3′ coterminal "nested set." In addition, each mRNA has a common leader sequence at its 5′ terminus, which is derived from the 5′ end of the genome (1, 9, 11, 34). Translation of different viral polypeptides is initiated independently (26, 27). Several studies have shown that mRNA7, mRNA6, and mRNA3 encode the virion nucleocapsid protein (NP), the matrix protein (E1), and the precursor of peplomer protein (E2), respectively (16, 25, 27, 29).

Defective interfering (DI) particles are deletion mutants which cannot replicate by themselves but interfere specifically with replication of the homologous virus, which is in turn required for the generation and replication of the DI particles. Many studies have focused on the role of DI virus genomes in virus evolution and in persistent infection. Although coronaviruses tend to establish persistent infection in tissue culture (30), in contrast to other positive-stranded viruses, there have been no reports about the isolation of coronavirus DI particles during persistent infection. The generation of coronavirus DI particles during high-multiplicity passages of the JHM strain of MHV (MHV-JHM) was recently reported (18). These DI particles differ from standard virus in that they contain a single positive-stranded RNA (molecular weight [mw], 5.2 × 10^6) which is smaller than the genomic RNA of the standard virus (mw, 5.4 × 10^6). Oligonucleotide fingerprinting studies indicated that the RNA of MHV-JHM DI particles had lost several large RNase T_1-resistant oligonucleotides. In the experiments in this study, we further examined the RNA synthesis in the DI-infected cells. We identified seven novel polyadenylic acid-containing intracellular DI-specific RNAs, which were generated at different times during undiluted passage of the virus. Using oligonucleotide fingerprinting, we have shown that these DI RNAs contain multiple deletions. Furthermore, the synthesis of six of the seven MHV-JHM-specific genomic and subgenomic RNAs was inhibited after infection with late-passage viruses. Interestingly, the synthesis of RNA7 and its product NP was not inhibited. The possible mechanism for the synthesis of these DI RNAs is discussed.

MATERIALS AND METHODS

Virus and cell culture. The standard MHV-JHM and serially passaged viruses were grown on DBT cells (mouse cell line transformed by the Schmidt-Ruppin strain of Rous sarcoma virus) (7) as described previously (18).

Preparation of intracellular viral RNA. ^{32}P-labeled intracellular viral RNA was extracted by procedures described previously (21). Briefly, a monolayer culture of DBT cells was infected with viruses at a multiplicity of infection of 1.0 and labeled with $^{32}P_i$ from 6 to 9 h postinfection in the presence of 2.5 μg of actinomycin D per ml. Cytoplasmic extracts were prepared by lysing the cells in NTE buffer (0.1 M NaCl, 0.01 M Tris-hydrochloride [pH 7.2], 1 mM EDTA) containing 0.5% Nonidet P-40. RNA was isolated by phenol-chloroform extractions as described previously (18).

Agarose gel electrophoresis. Analytical gel electrophoresis was conducted after denaturation of RNA with glyoxal treatment as described previously (22). Preparative gel electrophoresis in 1% urea–agarose gel was performed by published procedures (18). Each RNA species was purified by two cycles of urea-agarose gel electrophoresis to avoid contamination of smaller-sized RNAs. The RNA was eluted

* Corresponding author.
† Present address: Department of Microbiology, School of Medicine, University of Southern California, Los Angeles, CA 90033.

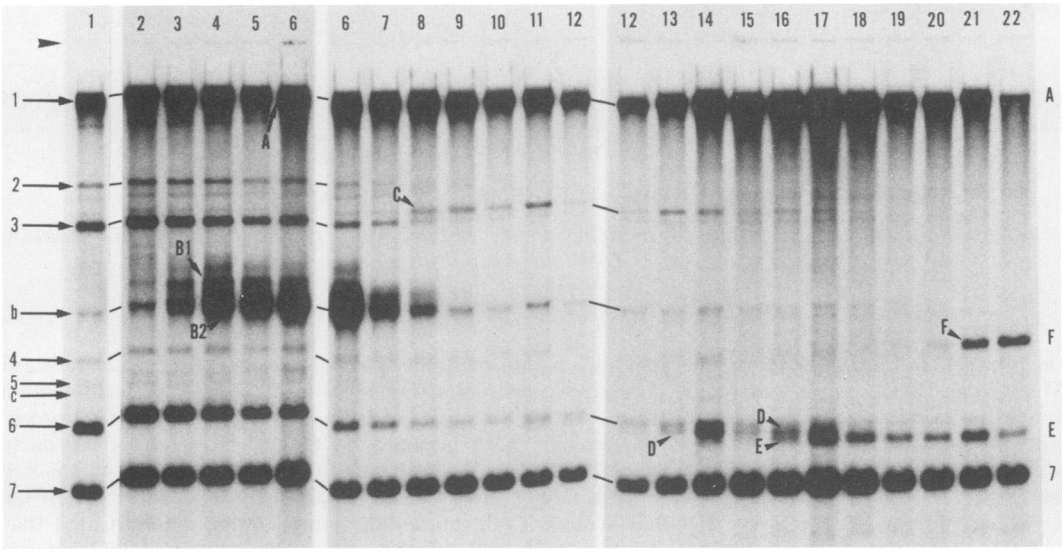

FIG. 1. Agarose gel electrophoresis of glyoxal-denatured intracellular RNAs from different passage levels. The RNAs extracted from each culture were denatured with glyoxal-dimethyl sulfoxide and electrophoresed on 1% agarose gels. The arrowhead indicates the top of the lanes. The number over each lane denotes the passage level of the virus propagated in the cells, e.g., no. 9 denotes passage 8 virus as the virus inoculum, and capital letters represent the species of DI RNA. The intracellular RNA species of the standard MHV-JHM are denoted on the side of the gel (21).

from gel slices by the method of Langridge et al. (13). If the urea-gel was to be dried as a film, urea was first removed by soaking the gel in 0.1 M ammonium acetate for at least 2 h with a change of buffer. Kodak XAR-5 film with an intensifying screen was used for autoradiography.

Oligonucleotide fingerprinting. Two-dimensional polyacrylamide gel electrophoresis was performed as previously described (18).

Labeling of intracellular proteins. Monolayers of cells (6×10^5 cells) were infected with viruses at a multiplicity of infection of 1.0. After virus adsorption, cultures were incubated with Eagle minimal essential medium containing 5% dialyzed calf serum. At 10 h postinfection, the cultures were treated with medium lacking leucine and serum for 15 min, and then the same medium containing 100 μCi of [^{3}H]leucine (55.5 Ci/mmol; Amersham Corp.) per ml was added. The cells were pulse-labeled for 10 min, chilled on ice, washed twice with chilled phosphate-buffered saline (pH 7.2), and lysed with 300 μl of lysis buffer (1% Triton X-100, 0.5% sodium deoxycholate, 0.1% sodium dodecyl sulfate [SDS] in phosphate-buffered saline) containing 1 mM phenylmethylsulfonyl fluoride. The cell lysate was immediately passed through a syringe needle 5 times and centrifuged at 12,000 × *g* for 10 min at 4°C. The supernatant fluid was stored at −70°C.

Immunoprecipitation and gel electrophoresis. A 50-μl volume of each cytoplasmic lysate was incubated with 5 μl of rabbit hyperimmune serum against purified MHV-JHM at 0 to 4°C for 2 h (19). Formalin-fixed *Staphylococcus aureus* (10% suspension in lysis buffer; 50 μl per reaction) was then added to the reaction mixture which was further incubated at 0 to 4°C for 2 h. The precipitates were collected by centrifugation at 4,000 × *g* for 3 min and washed three times with lysis buffer. The final pellet was suspended in sample buffer (0.06 M Tris-hydrochloride [pH 6.8], 2% SDS, 25% glycerol, 5% 2-mercaptoethanol, 0.1% bromophenol blue), heated at 100°C for 2 min, and centrifuged at 6,000 × *g* for 3 min. The supernatants were electrophoresed on 7.5 to 15% SDS-polyacrylamide gel (8, 20). The gels were further processed for fluorography with sodium salicylate (4).

RESULTS

Intracellular viral RNA species produced by serial undilute-passaged viruses. Previously it was shown that the DI particles obtained from the serial undiluted passages of MHV-JHM contain an RNA species slightly smaller than the genomic RNA of standard virus (18). To determine whether the cells infected with these DI particles also contain intracellular viral subgenomic RNAs of a smaller size, we analyzed by agarose gel electrophoresis the virus-specific RNA from the cells infected with undiluted viruses at different passage levels (Fig. 1). As previously reported (21), two minor RNA species, RNA b and c, in addition to the seven major mRNA species in the standard MHV-JHM-infected cells, were consistently detected. It appears that the synthesis of all of the MHV-JHM-specific mRNAs, except RNA7, was inhibited in the cells infected with the late-passage viruses. The degree of inhibition corresponded to the level of virus passage. Also, every viral mRNA species, except RNA7, was inhibited roughly to the same extent. Furthermore, several new RNA species, termed DIssA through DIssF, were detected in the cells infected with virus at various passage levels. The largest new intracellular RNA species, DIssA RNA, appears to correspond to the viral genomic RNA species packaged in the DI particles (DI-P RNA) (18). Since the resolution of DIssA and genomic RNA was poor in the agarose gel under these conditions, we further analyzed these RNAs by urea-agarose gel electrophoresis (18) (Fig. 2). DIssA could be clearly separated from RNA1 of the standard virus. It is also noteworthy that DIssB1 and DIssB2 RNAs migrated differently under these two different electrophoretic conditions. The mw's of these new RNA species were determined from glyoxal-agarose gels as follows: A; 5.2×10^6, B1; 1.9×10^6 to 1.6×10^6, B2; 1.6×10^6, C; 2.8×10^6, D; 0.82×10^6, E; 0.78×10^6, F; 1.3×10^6. DIssC appears to migrate together with RNA3 in

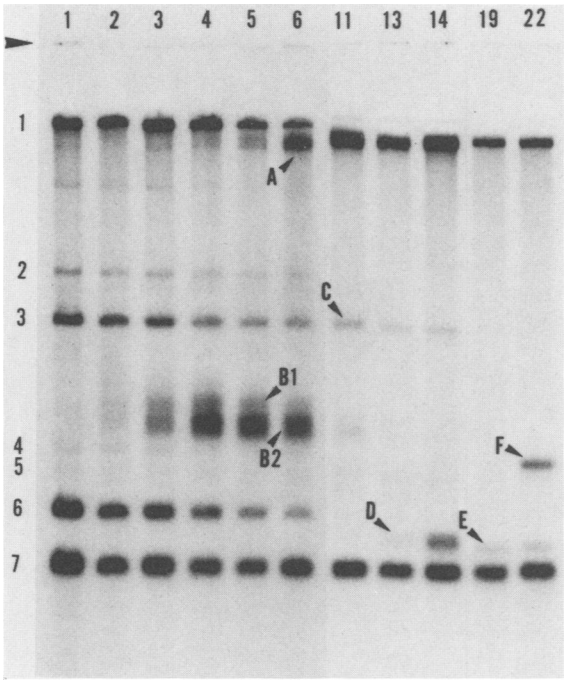

FIG. 2. Urea-agarose gel electrophoresis of intracellular RNAs from different passage levels. Ethanol-precipitated RNA was dissolved in 10 mM sodium phosphate (pH 7.0), containing 1 mM EDTA, 0.1% SDS, 0.1% bromophenol blue, and 0.1% xylene cyanol FF, and mixed with an equal volume of glycerol. The solution was heated for 5 min at 56°C, rapidly cooled on ice, and applied to a horizontal 1% agarose gel in electrophoresis buffer (40 mM Tris, 20 mM sodium acetate, 33 mM acetic acid, 2 mM EDTA [pH 7.4]) supplemented with 6 M deionized urea. Electrophoresis was performed at 4°C. After electrophoresis, urea was removed by soaking the gel in 0.1 M ammonium acetate before the gel was dried under vacuum.

urea-agarose gels; however, they were clearly separated in glyoxal-agarose gels (Fig. 1) and nondenaturing gels (data not shown). Oligodeoxythymidylic acid-cellulose column chromatography and RNase A digestion studies indicated that all of these RNA species were polyadenylated and single stranded (data not shown).

Sequence relationships of the DI RNAs. To determine the sequence relationships and structures of these newly synthesized RNAs, we examined each DI RNA by RNase T_1-oligonucleotide fingerprinting. ^{32}P-labeled polyadenylic acid-containing intracellular viral RNAs from different passage levels were separated by repeated electrophoresis on urea-agarose gels. After the second electrophoresis, the contamination of other RNA species in each intracellular viral RNA was no longer detected. Each purified DI-specific RNA was isolated from gels, digested with RNase T_1, and separated by two-dimensional polyacrylamide gel electrophoresis. The oligonucleotide fingerprints of the standard MHV-JHM genomic RNA and of DIssA RNAs from passage levels 10 and 22 are shown (Fig. 3). It can be seen that both DIssA RNAs are very similar to the standard MHV-JHM genomic RNA, but both lack 16 distinct large T_1-oligonucleotides present in the MHV-JHM genome (the spots indicated by open circles in Fig. 3B and C). This result is consistent with the interpretation that DIssA RNAs are derived from deletion of the MHV-JHM genomic RNA. Both DIssA RNAs also contain two additional oligonucleotides (indicated by arrows in Fig. 3) not found in the MHV-JHM genome. Furthermore, oligonucleotides 2b and 7 (indicated by arrowheads in Fig. 3B and C) which are detected in the MHV-JHM genomic RNA are also present as minor spots in both DIssA RNAs. The differences in the oligonucleotide fingerprint patterns of MHV-JHM genomic RNA and DIssA RNA are summarized (Fig. 4). The numbering of oligonucleotides was done by the methods of previous studies (18, 21, 35).

DIssB1 and DIssB2 of passage 6, DIssC and DIssD of passage 13, DIssE and DIssF of passage 22, and RNA7 (passages 1 and 13) also were analyzed by oligonucleotide fingerprinting (Fig. 5). All of the oligonucleotides were given the same numbers as the corresponding spots in MHV-JHM genomic RNA (Fig. 4). It became clear that all of these DI-specific RNAs contain subsets of the oligonucleotides present in the DIssA RNA and MHV-JHM genomic RNA. Some of them also contain a few minor spots (indicated by arrows) which are not present in the MHV-JHM genome. Furthermore, these DI RNAs are related to each other. Most of the oligonucleotides present in the smaller DI RNAs are

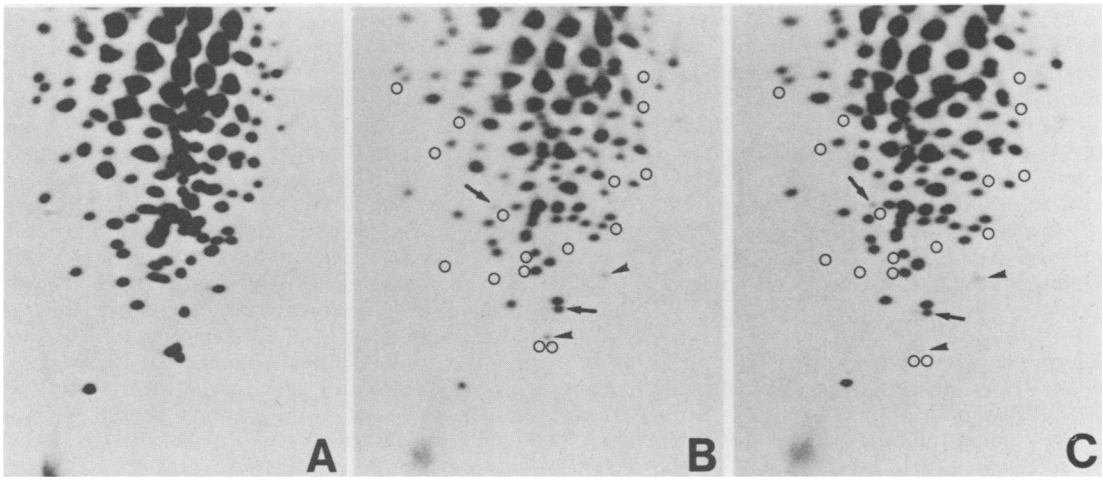

FIG. 3. Oligonucleotide fingerprints of the genomic RNA of MHV-JHM (A) and DIssA RNAs of passages 10 (B) and 22 (C). Open circles in B and C denote the oligonucleotide spots detected only in MHV-JHM genomic RNA. Arrows in B and C denote the oligonucleotide spots found only in DIssA. Arrowheads in B and C indicate the minor oligonucleotide spots found in DIssA.

subsets of the oligonucleotides present in the larger DI RNAs. All the oligonucleotides present in DIssE, except for one spot (indicated by an arrow), were present in all other DI RNAs. It is noteworthy that the subsets of oligonucleotides contained in DI RNAs are different from those contained in RNA7 (Fig. 5G and H) or any other subgenomic mRNAs of the standard MHV-JHM (21). Thus, these RNAs are novel DI-specific RNAs. Also, the fingerprint patterns of RNA7 at passage levels of 13 and 22 (data not shown) are identical to that of the original MHV-JHM RNA7.

Since the map positions of most of the oligonucleotides in the MHV-JHM genome have been determined (21), it is possible to determine the sequence relationship between each DI RNA and the standard virus genome by comparing their oligonucleotide maps (Fig. 6). DIssA had lost a number of oligonucleotides at a region of 2 to 8.7 kilobases from the 3′ end of the genomic RNA of MHV-JHM. Another oligonucleotide also was lost at a region of 11 to 14.8 kilobases from the 3′ end of the genome. It is noteworthy that all of the oligonucleotides lost from the DIssA RNA are not contiguous on the MHV-JHM genome, suggesting that DIssA has not undergone a single internal deletion but rather contained multiple deletions. All of the oligonucleotides of DIssE, which are common to all of the DI RNAs, are localized within either 3′ or 5′ ends of the genome. This result suggests that DIssE has undergone multiple deletions at both ends of the genome, in addition to an internal deletion of nearly 10 kilobases. The oligonucleotides of other DI RNAs also were scattered throughout the genome, suggesting that they have undergone multiple deletions. We cannot, however, rule out the possibility that these RNAs might have other mutations or sequence rearrangements besides simple multiple deletions (see below).

Synthesis of MHV-JHM-specific intracellular structural proteins by infection with serially passaged viruses. The studies described above indicated that the synthesis of genomic and subgenomic RNA of MHV-JHM, except for RNA7, was decreased after infection with late-passage viruses. To determine whether translation of RNA7 was inhibited by infection with late-passage viruses, synthesis of the MHV-JHM-specific proteins in the infected cells was examined. DBT cells were mock infected or infected with viruses from passage 0, 5, 13, 18, or 21 at a multiplicity of infection of 1.0. The infected cells were pulse-labeled with [^{3}H]leucine. The cytoplasmic lysate was immunoprecipitated with serum against purified MHV-JHM virions and subjected to SDS-polyacrylamide gel electrophoresis analysis (Fig. 7). Three major polypeptides with mw's of 150,000 (150K), 60K, and 21K, representing the precursor proteins of E2, NP, and E1, respectively (26), were detected in the cells infected with the original MHV-JHM or early-passage viruses. The synthesis of the 150K and 21K proteins was significantly reduced after infection with late-passage viruses (passages 14 to 22); however, NP synthesis was not suppressed. These results indicate that synthesis of RNA7 and its product NP was resistant to inhibition by late-passage-level viruses.

DISCUSSION

In this report we identified seven different species of intracellular DI RNAs and examined their structural relationship by oligonucleotide fingerprinting. We found that these DI RNAs contain multiple deletions of the genomic RNA. We also showed that levels of six of the seven MHV-JHM-specific mRNAs were reduced in cells infected with DI particles but that synthesis of RNA7 and its product NP was not inhibited.

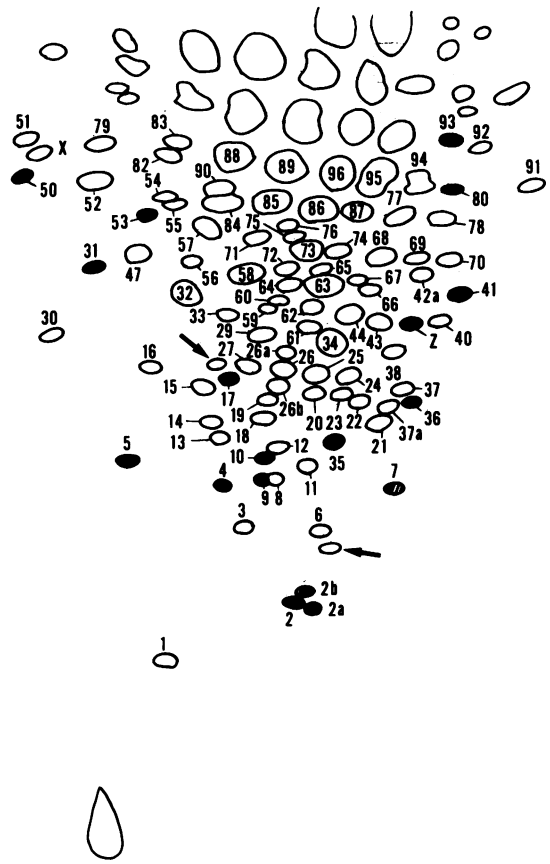

FIG. 4. Diagrammatic representation of the relationships between the oligonucleotide fingerprints of MHV-JHM genomic RNA and DIssA. The numbering of oligonucleotides is by the methods described in previous studies (18, 21, 35). Closed spots denote the oligonucleotide spots detected only in MHV-JHM genomic RNA. Arrows denote the oligonucleotide spots found in DIssA. Cross-hatched spots denote the minor oligonucleotide spots found in DIssA.

The DIssA RNA and DI-P RNA have identical mw's and similar oligonucleotide fingerprint patterns (18). Therefore, it is likely that the DIssA was packaged into DI particles. However, there were some observed differences between DIssA and DI-P RNAs. DI-P RNA contains several minor oligonucleotides which are not detected in DIssA (18). Also, DIssA contained two minor oligonucleotide spots. This result suggests that both DIssA and DI-P RNAs are heterogeneous. It is possible that some minor RNA species are packaged into DI particles more efficiently than others. The identification of sequences required for packaging of RNA will be very important.

Our oligonucleotide fingerprinting study suggests that every DI RNA seems to have undergone multiple deletions. However, different DI RNAs might have been generated by mechanisms other than simple deletions. DIssA, DIssD, and DIssE may have resulted from simple deletions, since the number of detectable oligonucleotide spots in these DI RNAs is about the same as that in the MHV-JHM subgenomic RNAs of corresponding size (21). However, the number of oligonucleotides in DIssB (DIssB1 and DIssB2) was only half of that in RNAb which possesses a similar mw to that of DIssB. DIssC and DIssF also contained considerably fewer oligonucleotides than did the MHV-JHM subgenomic RNAs of corresponding sizes. Recent studies indicate

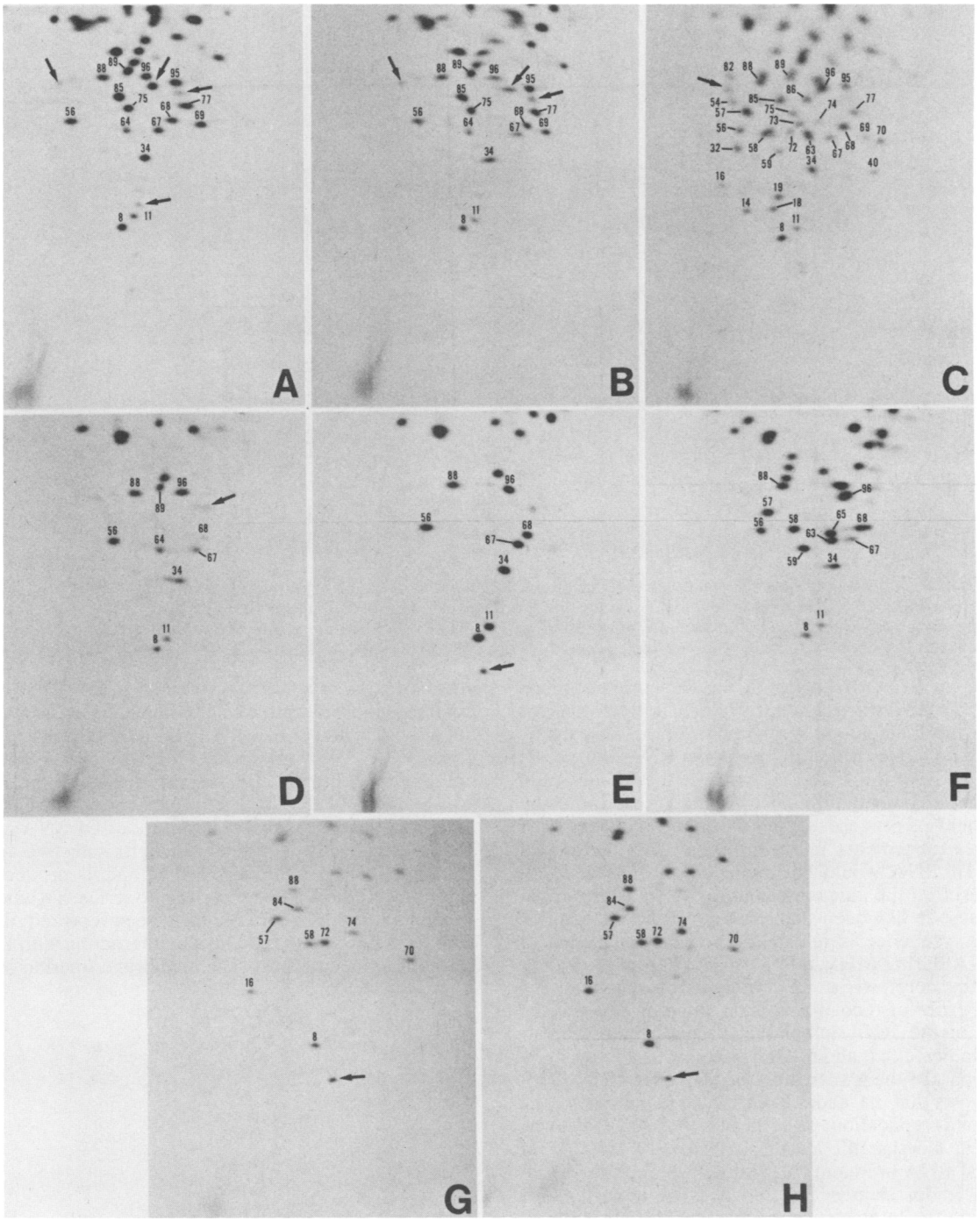

FIG. 5. Oligonucleotide fingerprints of DIssB1 (A) and DIssB2 (B) of passage 6, DIssC (C) and DIssD (D) of passage 13, DIssE (E) and DIssF (F) of passage 22, and RNA7 of original MHV-JHM (G) and of passage 13 (H). Arrows indicate the oligonucleotide spots which are not present in MHV-JHM genomic RNA.

that several alpha virus DI RNAs contain sequence duplications, triplications, and rearrangements in addition to deletions (5, 14, 15, 23, 24, 33). Similar structures might be present in MHV-JHM DI RNAs. The possible presence of multiple deletions and sequence rearrangements could also explain the occurrence of unique oligonucleotides in each DI RNA which are not found in other DI RNAs. Oligonucleotide fingerprint patterns of DIssB1 and DIssB2 were almost identical, but DIssB1 showed diffuse RNA bands (Fig. 1), suggesting that DIssB1 represented a heterogeneous population with minor differences in gene sequences. Similar results also were reported for DI RNAs of other viruses (5, 6, 24).

The most exciting aspect of this study is that these DI RNAs are present only in the infected cells and are not packaged in the DI particles (18). The smaller DI RNAs are probably not packaged since they might lack packaging signals or, alternatively, there may be a minimum size

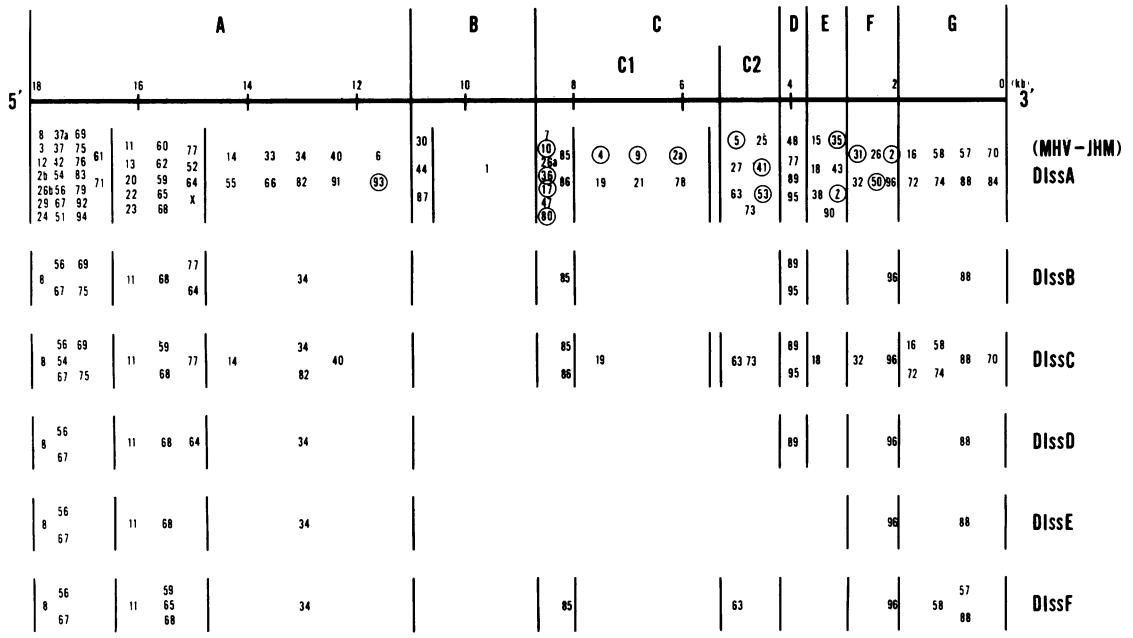

FIG. 6. Comparison of oligonucleotide maps of the various DI RNAs. The order of oligonucleotides within each region separated by vertical lines is arbitrary. The proposed seven genetic regions are based on data described previously (10, 21, 27). Numbers which are surrounded by circles represent the spots which are not present in DIssA but which are present in MHV-JHM genomic RNA.

requirement for RNA packaging. If the DI particles indeed do not contain any trace amount of the DI RNA species detected in the infected cells, these DI RNAs have to be synthesized de novo from the genomic RNA of the DI particles, i.e., DI-P RNA. In other words, the sequences in the DI-P RNA could determine how the transcription by RNA polymerases proceeds, generating specific deletions or sequence rearrangements in the process. This method of generating DI RNA would be unique to coronaviruses. It may be a result of the unique mechanism of transcription of coronaviruses. It has been demonstrated that a stretch of leader RNA sequence is joined to the body sequence of every mRNA during MHV mRNA transcription (1, 9, 34). Therefore the coronavirus RNA polymerases might have unique properties of recognizing and "jumping" to specific sequences on the RNA template. Present studies in our laboratory indicate that all DI RNAs contain oligonucleotide 8, which is part of the leader RNA of MHV-JHM (21). This finding suggests that the leader RNA is also important for the transcription or replication, or both, of DI RNAs. However, it is not clear whether the leader sequences of MHV-JHM RNA and DI RNA are identical. Further comparative studies of each leader sequence would be very important for understanding the interference mechanisms by DI particles (see below). It also should be noted that all major oligonucleotides present in DIssE were common to other DI RNA species. DIssE might possess essential sequences for the transcription of DIss RNA and standard virus mRNA. Therefore, sequence analysis of DIssE RNA will provide very valuable information concerning the sequence requirement of leader-body fusion signals.

The present study clearly indicates that the interference of standard MHV-JHM replication occurred before or at RNA transcription. One possible mechanism of interference by MHV DI particles is through competition between standard virus RNA and DI RNA for the viral polymerase. If the efficiency of replication for DI RNA is identical to that for standard viral RNA, the synthesis of DI RNA would be favored simply because of its smaller size. However, the difference in mw between DIssA and standard MHV-JHM genomic RNA is very small. Therefore, RNA size alone is not likely to be directly responsible for the competitive advantage of DI RNAs. The primary, secondary, or tertiary (or a combination of these) structure of DI RNA might play a more decisive role in determining its selective advantage.

Interestingly, synthesis of RNA7 and its product NP was not inhibited throughout the passage series. To date, several characteristic features of NP have been reported, namely, (i) binding to genomic RNA (38), (ii) interacting with E1 protein (38), (iii) association with the membrane fraction of infected

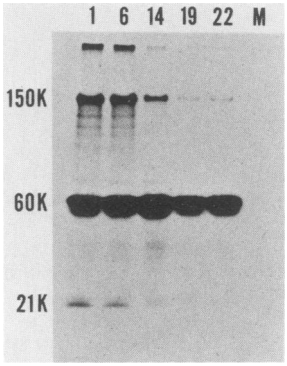

FIG. 7. Electrophoretic analysis of the virus-specific proteins in cells infected with MHV-JHM at different passage levels. DBT cells were mock infected (lane M) or infected with original MHV-JHM (lane 1), passage 5 virus (lane 6), passage 13 virus (lane 14), passage 18 virus (lane 19), or passage 21 virus (lane 22). At 10 h postinfection, cultures were pulse-labeled with [^{3}H]leucine, and cytoplasmic lysates were prepared, immunoprecipitated with anti-JHM serum, and electrophoresed as described in the text.

cells (36), and (iv) phosphorylation of serine residues (37), presumably by a virion-associated protein kinase (28). Present data suggest that the NP plays important roles in MHV RNA synthesis, DI RNA synthesis, or both. Fingerprinting studies indicate that DIssA and DI-P RNA have no deletions in the NP coding region (0 to 2 kilobases from the 3′ end of the genome) (32). Furthermore, our preliminary data show that the replicative-form RNA and the replicative intermediates in the cells infected with late-passage viruses consist of only one RNA species and that the replicative intermediates in the DI-infected cells electrophoresed slightly faster than the replicative intermediates in the original MHV-JHM-infected cells (S. Makino, unpublished data). No subgenomic replicative form and replicative intermediates were found. These results suggest that all of the DI-specific intracellular RNAs as well as RNA7 are transcribed from the same negative-stranded RNA of DI-P RNA of the DI particles, in a way similar to the synthesis of subgenomic RNAs of the standard virus (12). Further studies on the detailed structure of the DI RNAs are required for the understanding of the mechanism of transcription or replication, or both, of DI RNAs. Such studies are in progress.

ACKNOWLEDGMENTS

We thank Michael M. C. Lai and Ralph S. Baric for valuable discussion and correction of the manuscript and Y. Yoshikawa for his critical reading of the manuscript.

LITERATURE CITED

1. **Baric, R. S., S. A. Stohlman, and M. M. C. Lai.** 1983. Characterization of replicative intermediate RNA of mouse hepatitis virus: presence of leader RNA sequences on nascent chains. J. Virol. **48**:633–640.
2. **Brayton, P. R., M. M. C. Lai, C. D. Patton, and S. A. Stohlman.** 1982. Characterization of two RNA polymerase activities induced by mouse hepatitis virus. J. Virol. **42**:847–853.
3. **Brayton, P. R., S. A. Stohlman, and M. M. C. Lai.** 1984. Further characterization of mouse hepatitis virus RNA-dependent RNA polymerases. Virology **133**:197–201.
4. **Chamberlain, J. P.** 1979. Fluorographic detection of radioactivity in polyacrylamide gels with the water-soluble flour, sodium salicylate. Anal. Biochem. **98**:132–135.
5. **Dohner, D., S. Monroe, B. Weiss, and S. Schlesinger.** 1979. Oligonucleotide mapping studies of standard and defective Sindbis virus RNA. J. Virol. **29**:794–798.
6. **Kennedy, S. I. T., C. J. Bruton, B. Weiss, and S. Schlesinger.** 1976. Defective interfering particles of Sindbis virus: nature of the defective virion RNA. J. Virol. **19**:1034–1043.
7. **Kumanishi, T.** 1967. Brain tumors induced with Rous sarcoma virus, Schmidt-Ruppin strain. I. Induction of brain tumors in adult mice with Rous chicken sarcoma cells. Jpn. J. Exp. Med. **37**:461–474.
8. **Laemmli, U. K.** 1970. Cleavage of structural proteins during the assembly of the head of bacteriophage T4. Nature (London) **227**:680–685.
9. **Lai, M. M. C., R. S. Baric, P. R. Brayton, and S. A. Stohlman.** 1984. Characterization of leader RNA sequences on the virion and mRNAs of mouse hepatitis virus, a cytoplasmic RNA virus. Proc. Natl. Acad. Sci. U.S.A. **81**:3626–3630.
10. **Lai, M. M. C., P. R. Brayton, R. C. Armen, C. D. Patton, C. Pugh, and S. A. Stohlman.** 1981. Mouse hepatitis virus A59: mRNA structure and genetic localization of the sequence divergence from hepatotropic strain MHV-3. J. Virol. **39**:823–834.
11. **Lai, M. M. C., C. D. Patton, R. S. Baric, and S. A. Stohlman.** 1983. Presence of leader sequences in the mRNA of mouse hepatitis virus. J. Virol. **46**:1027–1033.
12. **Lai, M. M. C., C. D. Patton, and S. A. Stohlman.** 1982. Replication of mouse hepatitis virus: negative-stranded RNA and replicative form RNA are of genome length. J. Virol. **44**:487–492.
13. **Langridge, L., P. Langridge, and P. L. Bergquist.** 1980. Extraction of nucleic acids from agarose gels. Anal. Biochem. **103**:264–271.
14. **Lehtovaara, P., H. Söderlund, S. Keränen, R. F. Pettersson, and L. Kääriäinen.** 1981. 18S defective interfering RNA of Semliki Forest virus contain a triplicated linear repeat. Proc. Natl. Acad. Sci. U.S.A. **78**:5353–5357.
15. **Lehtovaara, P., H. Söderlund, S. Keränen, R. F. Pettersson, and L. Kääriäinen.** 1982. Extreme ends of the genome are conserved and rearranged in the defective interfering RNAs of Semliki Forest virus. J. Mol. Biol. **156**:731–748.
16. **Leibowitz, J. L., S. R. Weiss, E. Paavola, and C. W. Bond.** 1982. Cell-free translation of murine coronavirus RNA. J. Virol. **43**:905–913.
17. **Mahy, B. M. J., S. Siddell, H. Wege, and V. ter Meulen.** 1983. RNA-dependent RNA polymerase activity in murine coronavirus-infected cells. J. Gen. Virol. **64**:103–111.
18. **Makino, S., F. Taguchi, and K. Fujiwara.** 1984. Defective interfering particles of mouse hepatitis virus. Virology **133**:9–17.
19. **Makino, S., F. Taguchi, K. Fujiwara, and M. Hayami.** 1982. Heterologous response of antiserum-treated cell clones from a persistently infected DBT cell line to mouse hepatitis virus. Jpn. J. Exp. Med. **52**:297–302.
20. **Makino, S., F. Taguchi, M. Hayami, and K. Fujiwara.** 1983. Characterization of small plaque mutants of mouse hepatitis virus, JHM strain. Microbiol. Immunol. **27**:445–454.
21. **Makino, S., F. Taguchi, N. Hirano, and K. Fujiwara.** 1984. Analysis of genomic and intracellular viral RNAs of small plaque mutants of mouse hepatitis virus, JHM strain. Virology **139**:138–151.
22. **McMaster, G. K., and G. G. Carmichael.** 1977. Analysis of single- and double-stranded nucleic acids on polyacrylamide and agarose gels by using glyoxal and acridine orange. Proc. Natl. Acad. Sci. U.S.A. **74**:4835–4838.
23. **Monroe, S. S., J.-H. Ou, C. M. Rice, S. Schlesinger, E. G. Strauss, and J. H. Strauss.** 1982. Sequence analysis of cDNA's derived from the RNA of Sindbis virions and of defective interfering particles. J. Virol. **41**:153–162.
24. **Monroe, S. S., and S. Schlesinger.** 1984. Common and distinct regions of defective-interfering RNAs of Sindbis virus. J. Virol. **49**:865–872.
25. **Rottier, P. J. M., W. J. M. Spaan, M. C. Horzinek, and B. A. M. van der Zeijst.** 1981. Translation of three mouse hepatitis virus strain A59 subgenomic RNAs in *Xenopus laevis* oocytes. J. Virol. **38**:20–26.
26. **Siddell, S.** 1982. Coronavirus JHM: tryptic peptide fingerprinting of virion proteins and intracellular polypeptides. J. Gen. Virol. **62**:259–269.
27. **Siddell, S.** 1983. Coronavirus JHM: coding assignments of subgenomic mRNAs. J. Gen. Virol. **64**:113–125.
28. **Siddell, S. G., A. Barthel, and V. ter Meulen.** 1981. Coronavirus JHM: a virion-associated protein kinase. J. Gen. Virol. **52**:235–243.
29. **Siddell, S. G., H. Wege, A. Barthel, and V. ter Meulen.** 1980. Coronavirus JHM: cell-free synthesis of structural protein p60. J. Virol. **33**:10–17.
30. **Siddell, S. G., H. Wege, and V. ter Meulen.** 1982. The structure and replication of coronaviruses. Curr. Top. Microbiol. Immunol. **99**:131–163.
31. **Siddell, S. G., H. Wege, and V. ter Meulen.** 1983. The biology of coronaviruses. J. Gen. Virol. **64**:761–776.
32. **Skinner, M. A., and S. G. Siddell.** 1983. Coronavirus JHM: nucleotide sequence of the mRNA that encodes nucleocapsid protein. Nucleic Acids Res. **11**:5045–5054.
33. **Söderlund, H., S. Keränen, P. Lehtovaara, I. Palva, R. F. Pettersson, and L. Kääriäinen.** 1981. Structural complexity of defective-interfering RNAs of Semliki Forest virus as revealed by analysis of complementary DNA. Nucleic Acids Res. **9**:3403–3417.
34. **Spaan, W., H. Delius, M. Skinner, J. Armstrong, P. Rottier, S. Smeekens, B. A. M. van der Zeijst, and S. G. Siddell.** 1983. Coronavirus mRNA synthesis involves fusion of non-contiguous sequences. EMBO J. **2**:1939–1944.

35. **Stohlman, S. A., P. R. Brayton, J. O. Fleming, L. P. Weiner, and M. M. C. Lai.** 1982. Murine coronaviruses: isolation and characterization of two plaque morphology variants of the JHM neurotropic strain. J. Gen. Virol. **63**:265–275.
36. **Stohlman, S. A., J. O. Fleming, C. D. Patton, and M. M. C. Lai.** 1983. Synthesis and subcellular localization of the murine coronavirus nucleocapsid protein. Virology **130**:527–532.
37. **Stohlman, S. A., and M. M. C. Lai.** 1979. Phosphoproteins of murine hepatitis viruses. J. Virol. **32**:672–675.
38. **Sturman, L. S., K. V. Holmes, and J. Behnke.** 1980. Isolation of coronavirus envelope glycoproteins and interaction with the viral nucleocapsid. J. Virol. **33**:449–462.